Supporting Information:

Bimetallic MOFs-derived MnCo spinel oxide catalyst to enhance toluene catalytic degradation

Bin Gao [a] ‡, Fukun Bi [a, b] ‡, Zhuoxuan Zhou [a], Yaofei Zhang [a], Jiafeng Wei [a], Xutian Lv [a], Baolin Liu [b], Yuandong Huang [a], Xiaodong Zhang [a, c] *

[a] *School of Environment and Architecture, University of Shanghai for Science and Technology, Shanghai 200093, China*

[b] *School of Health Science and Engineering, University of Shanghai for Science and Technology, Shanghai 200093, China*

[c] *Shanghai Non-carbon Energy Conversion and Utilization Institute, Shanghai 200240, China*

* To whom correspondence should be addressed. Tel. +86 15921267160, Fax. +86 021 55275979
E-mail address: fatzhxd@126.com (X.D. Zhang)

‡ These authors contributed equally to this work.

Text S1 Catalysts preparation

Chemicals and materials: Manganese nitrate tetrahydrate ($Mn(NO_3)_2·4H_2O$, AR), cobalt nitrate hexahydrate ($Co(NO_3)_2·6H_2O$, AR), 1, 3, 5-phthalic acid (H_3-BTC, AR), absolute ethyl alcohol (99.7%) and N, N-dimethylformamide (DMF, AR) were purchased from Sinopharm Chemical reagent Co., LTD. All of the chemicals were used directly without any purification.

Synthesis of the Mn/Co-MOFs precursors: The Mn/Co-MOFs were prepared via a modified solvothermal method followed our previous work.[1] The detailed synthesis processes were as follows. Typically, 2.51 g of $Mn(NO_3)_2·4H_2O$ (10 mmol), 2.91 g of $Co(NO_3)_2·6H_2O$ (10 mmol) and 4.2 g of H_3-BTC (20 mmol) were dissolved in a mixture of 140 mL DMF and ethanol with a volume ratio of 1:1 under stirring (the molar ratio of Mn to Co was 1:1). After complete dissolution, the above mixture solution was transferred into the reaction reactor and crystalized in an oven at 120 °C for 24 h. After cooling to the environmental temperature, the powder was obtained via centrifuging, washing with ethanol for several times, and drying at 80 °C for 12 h. The obtained powder was named as 1Mn1Co-MOF. Additionally, the Mn/Co-MOFs with the molar ratio of Mn to Co of 4:1, 2:1, 1:2 and 4:1 named as 4Mn1Co-MOF, 2Mn1Co-MOF, 1Mn2Co-MOF and 1Mn4Co-MOF were also prepared via the same process, respectively.

Synthesis of the MnCox catalysts: The MnCoOx catalysts were prepared via calcination methods by using Mn/Co-MOFs with the sacrificial templates followed our previous work.[2] Generally, the Mn/Co-MOFs were firstly calcinated at 300 °C with a

heating rate of 5 °C/min under Ar atmosphere for 2 h. After cooling to the room temperature, the samples were furtherly calcinated under 30% O_2/Ar atmosphere at 300 °C for another 2 h. After that, the black powder named 4Mn1Co, 2Mn1Co, 1Mn1Co, 1Mn2Co and 1Mn4Co were obtained by using 4Mn1Co-MOF, 2Mn1Co-MOF, 1Mn1Co-MOF, 1Mn2Co-MOF and 1Mn4Co-MOF as the precursors, respectively. The Mn/Co molar ratio of 4Mn1Co, 2Mn1Co, 1Mn1Co, 1Mn2Co and 1Mn4Co detected by inductively coupled plasma optical emission spectrometer (ICP-OES) were 3.92, 2.24, 1.12, 0.49 and 0.26, respectively. Additionally, the 1Mn1Co-MOF was calcinated at 200, 300, 400 and 500 °C to obtain 1Mn1Co-200, 1Mn1Co-300, 1Mn1Co-400 and 1Mn1Co-500, respectively, to investigate the effect of calcination temperature on the catalytic performance.

Text S2 Detailed information of the characterizations

X-ray diffraction (XRD): The XRD patterns were detected on a Bruker D8 Advance X-ray diffractometer using a Cu Kα (40 kV, 40 mA) radiation monochromatic detector with a scan rate of 5°/min, scanning range of 10°∼80°.

Fourier transform infrared spectroscopy (FT-IR): The FT-IR spectra were collected in Nicolet iS50 (Thermo Fisher, America) with a resolution ratio of 4 and scan times of 64.

N_2 adsorption-desorption curves: The specific surface area and pore properties of the catalysts were determined by N_2 adsorption-desorption at 77 K (liquid nitrogen temperature) on a Quantachrome autosorb-iQ-2MP apparatus. Before analysis, the samples were outgassed under vacuum at 105 °C for 12 h to purification. The Brunauer-

Emmett-Teller (BET) model was utilized to calculate the specific surface area, and the pore size distributions were generated by Barrett-Joyner-Halenda (BJH) method.

X-ray photoelectron spectroscopy (XPS): XPS was performed on THERMO ESCALAB 250XZ. The binding energies were calibrated internally by the carbon deposit C1 s at 284.8 eV.

Scanning electronic microscopy (SEM): The Scanning electron microscopy (SEM) images were got on the Hitachi S-4800 after Au deposition with 20 kV accelerating voltage.

Transmission electron microscopy (TEM), high-resolution transmission electron microscopy (HRTEM) high-angle annular dark field (HAADF) and the corresponding element mapping: TEM, HRTEM and HAADF mapping are obtained on FEI Talos F200S Super-X-ray energy disperse spectroscopy.

H_2 temperature programed reduction (H_2-TPR) and O_2 temperature programed desorption (O_2-TPD): H_2-TPR and O_2-TPD were carried out on ChemBET TPR/TPD chemisorption analyzer. For H_2-TPR, before test, the samples were pretreated under N_2 atmosphere at 150 °C for 1 h. After cooling to 50 °C, the gas was switched to 5.0 vol.% H_2/Ar, and the temperature programmed reduction began from 50 to 800 °C at a heating rate of 10 °C/min. For O_2-TPD, before test, 100 mg of samples were pretreated under 30.0 Vol% O_2/Ar atmosphere at 200 °C for 1 h. After cooling to the room temperature, the gas was switched to He and swept for 30 min. Then, the temperature programming was started at a rate of 10 °C/min from 30 to 900 °C under He flow.

Adsorption breakthrough experiments, *temperature programmed desorption (TPD) and temperature programmed oxidation (TPO)*: Before TPD and TPO procedures, the adsorption performance of the as-prepared catalyst was tested. For adsorption test, 1000 ppm toluene or 1000 ppm toluene + 5.0 vol.% H_2O balanced by Ar at a mass flow of 50 mL/min was introduced into the fixed-bed microreactor at 30 °C. 0.2 g sample was placed in the reactor tube. Before adsorption test, the samples were swept under Ar atmosphere at 100 °C for 1 h. the concentration of toluene was detected by an online gas chromatograph (GC, GC2060) with two flame ionization detectors (FID). After adsorption saturation, TPD or TPO procedures were carried out. Firstly, the adsorption saturated samples were swept under Ar atmosphere at 30 °C for 1 h to remove the physical adsorbed toluene on the surface. After that, the TPD program was started. The temperature was ramped from 30 to 400 °C at a rate of 2 °C/min under Ar atmosphere. The concentration of VOCs and CO_2 were measured by the sample GC instrument. For TPO procedure, the processes were similar to that of TPO, except the gas was switched to 5.0 vol.% O_2 balanced with Ar.

In-situ diffuse reflection Fourier transform infrared spectrometer (DRIFTS): The DRIFTS was performed on Nicolet iS50 (Thermo Fisher, America) equipped with Harrick in-situ cell is used to explore the mechanism of toluene catalytic combustion. About 50 mg catalyst is added into the hold of diffuse reflection cell. The sample is first pre-treatment under an Ar atmosphere at 250 °C for 1 h, and then cooled down to the ambient temperature. For adsorption test, the gas was switched to 20 % O_2/Ar, and DRIFTS of as-pretreated sample was taken as background. Then, 1000 ppm toluene

was introduced by 20 % O_2/Ar for 1 h, and the signal was collected. For oxidation test, after pre-absorbed toluene, the sample temperature rose to the target temperature and the signal was collected.

Text S2 Detailed information of the reaction kinetics and water-resistance test

Reaction kinetic: For the kinetic study, toluene oxidation under excessive oxygen should obey a first-order reaction mechanism for the toluene molecule, following the equation:

$$\ln k = -\frac{Ea}{RT} + \ln A \quad (1)$$

where k, Ea, and A refer to rate constant (s^{-1}), apparent activation energy (kJ/mol), and pre-exponential factor, respectively. R and T represent gas constant (J/(mol·K)) and corresponding temperature (K), respectively. Arrhenius plots derived from the formula (1) are applied to the calculation of Ea at lower conversion (less than 20%).

Water-resistance test: For the influence of water vapor (5.0 and 10 vol.%), at a certain temperature, the water vapor was introduced by an Ar flow. The amount of water vapor was calculated by our previous work.[3]

Table S1. Pore structure parameter of the $MnCoO_x$ samples.

Samples	ICP-OES [a]			BET (m^2/g) [b]	Pore volume (cc/g) [c]	Pore size (nm) [d]
	Mn (wt%)	Co (wt%)	Mn/Co molar ratio			
4Mn1Co	78.53	21.47	3.92	197	0.33	3.0-6.3
2Mn1Co	67.94	32.06	2.27	244	0.36	3.1-6.3
1Mn1Co	51.17	48.83	1.12	193	0.28	2.6-6.4
1Mn2Co	31.48	68.52	0.49	162	0.25	2.4-5.8
1Mn4Co	19.47	80.53	0.26	158	0.10	2.4-5.8

[a] Data of element content is determined by the ICP-OES.

[b] BET specific surface;

[c] Total pore volume measured at P/P_0 =0.99;

[d] The pore diameter calculated from the isotherm using the DFT method.

Table S2 The comparison of specific surface area of the Mn/Co-MOFs derived spinel catalysts with the reported MnCo bimetallic catalysts.

Catalysts	Preparation method	Structure	Specific area (m^2/g)	Ref.
CoMn6	MOFs-derivation	$MnCo_2O_{4.5}$ spinel	163	[4]
MnCo-U	Urea precipitation	Mixture of Co_3O_4 and MnO_2	127	[5]
MOF-CMO-400	MOFs-derivation	$CoMn_2O_4$ spinel	92.4	[6]
CMO-E0.5	MOFs-derivation	$[Co,Mn][Co,Mn]_2O_4$ spinel	82.3	[7]
2Mn1Co	Hydrothermal-calcination	$[Co,Mn][Co,Mn]_2O_4$ spinel	244	This work

Table S3 Surface chemical composition, H_2 consumption amount and O_2 desorption peak area of the Mn/Co-MOFs derived MnCoOx catalysts.

Samples	Surface chemical compositions			H_2 consumption	O_2 desorption
	Mn^{3+}/Mn^{4+}	Co^{3+}/Co^{2+}	O_{ads}/O_{lat}	(μmol/g)	amount (μmol/g)
4Mn1Co	0.90	0.60	0.39	794.8	91.2
2Mn1Co	1.30	0.99	0.58	1299.0	290.4
1Mn1Co	1.16	0.78	0.53	972.8	234.8
1Mn2Co	0.94	0.64	0.40	887.9	220.5
1Mn4Co	0.80	0.58	0.37	701.2	60.0

Table S4 Catalytic performance of the Mn/Co-MOFs derived catalysts for toluene oxidation.

Samples	Catalytic performance (°C)			Activation energy (kJ/mol)
	T_{10}	T_{50}	T_{90}	
4Mn1Co	223	255	276	135.1
2Mn1Co	206	229	245	85.2
1Mn1Co	215	250	264	125.1
1Mn2Co	220	253	270	132.2
1Mn4Co	233	258	283	149.2

Table S5 Comparison of the catalytic performance for toluene oxidation over 2Mn1Co with the reported catalysts.

Catalysts	Preparation method	WHSV (mL/(g·h))	Toluene concentration (ppm)	Performance T_{90} (°C)	Ref.
Mn3Co1 oxides	Agar-gel	60000	1000	252	[8]
5Co1Mn	Hydrothermal	60000	1000	247	[9]
CoMn-1	Coprecipitation	15000	1000	250	[10]
Co^{2+}/MnCoO	Calcination	12000	7000	252	[11]
Mn_1Co_1Ox	Coprecipitation	24000	4000	280	[12]
0.01Mn-0.01Co/CF	Electrodeposition	30000	978	251	[13]
2Mn1Co	MOFs-derivation	30000	1000	245	This work

Table S6 The assignment of characteristic adsorption peaks in in-situ DRIFTS spectra.

Position (cm^{-1})	Assignment	Characteristic of	Ref.
2374, 2308	/	CO_2	[14,15]
1598, 1512, 1399	The COO^- asymmetry and symmetry vibration of benzoate	Benzoate acid	[8,16]
1491, 1472	C-H vibration of aromatic ring	Benzene	[14]
1454, 1444	C=O vibration of -CHO	Benzaldehyde	[14,17,18]
1296	ν(C=O) stretching of cyclic anhydride	Maleic anhydride	[18,19]
1240, 1241	ν(C-O) stretching vibration of surface phenolate	Phenol	[20,21]
1012, 1043, 1095, 1130, 1178,1361	ν(C-O) stretching vibration of alkoxide species	Benzyl alcohol	[18,19]

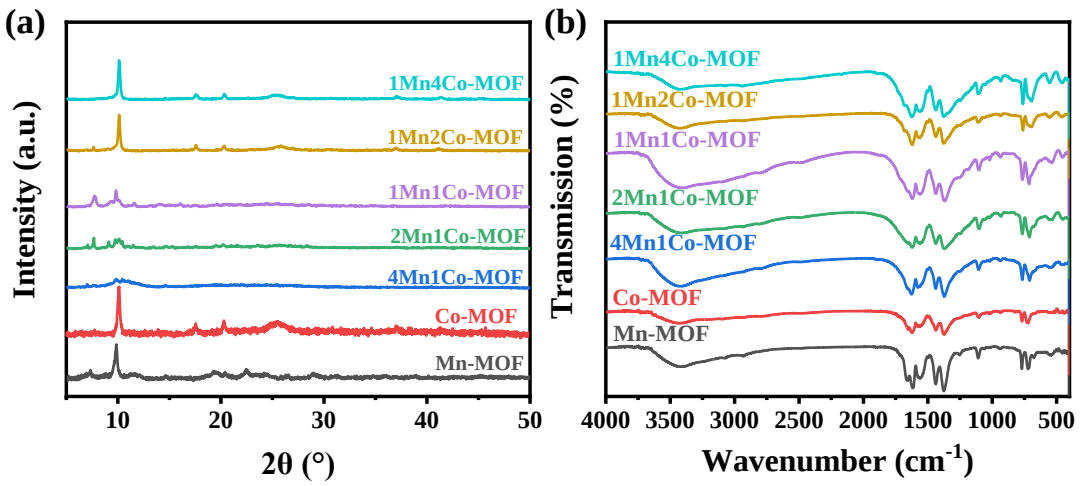

Fig. S1 XRD patterns (a) and FT-IR (b) of the Mn-MOF, Co-MOF and Mn/Co-MOFs.

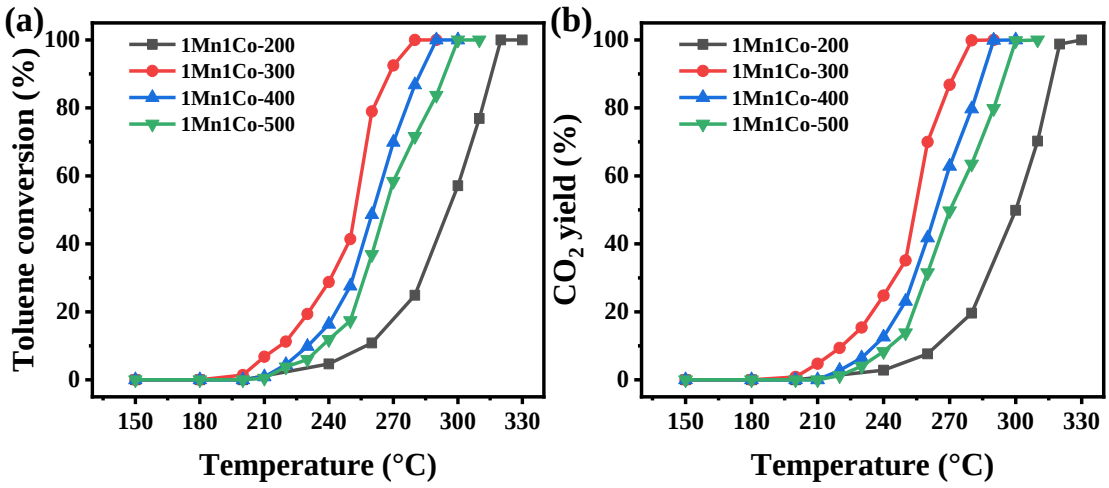

Fig. S2 Effect of calcination temperature on 1Mn1Co-MOF derived 1Mn1Co catalysts for toluene oxidation.

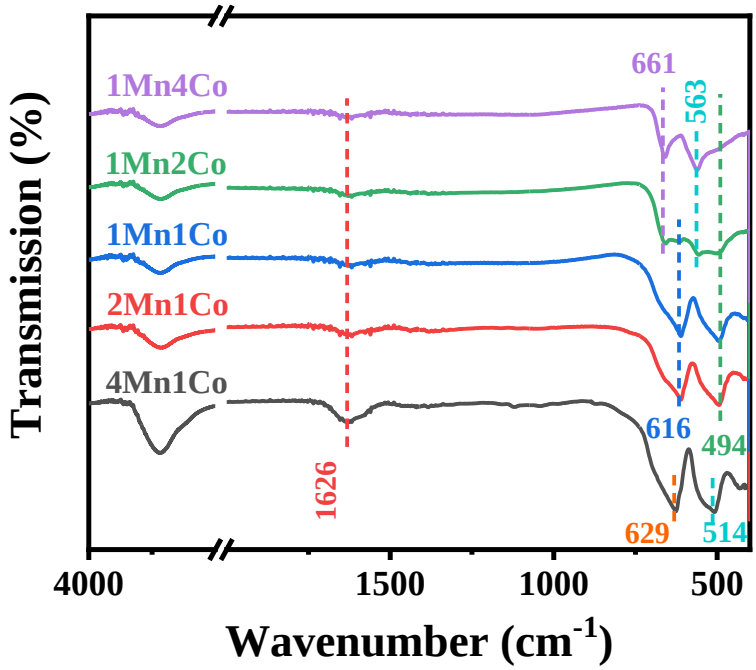

Fig. S3 FT-IR spectra of the MOFs-derived catalysts.

Fig. S3 presented the FT-IR spectra of the MOFs-derived catalysts. The vibration band at 1626 cm^{-1} was ascribed to the H_2O deformation vibration from the surface absorbed moisture in the catalysts surface.[22] Metal-oxygen bands were observed at 400-800 cm^{-1}. Bands at 629 and 514 cm^{-1} were attributed to the tetrahedral and octahedral Mn-O bands vibration of Mn_3O_4.[23] Bands at 616 and 494 cm^{-1} were assigned to the metal-oxygen band with different coordination environmental in $[Co,Mn][Co,Mn]_2O_4$ and $MnCo_2O_4$.[24] Two other bands at 661 and 563 cm^{-1} were ascribed to the stretching vibration of tetrahedral and octahedral Co-O bands in Co_3O_4, respectively.[24] Apparently, with the increase of Co molar ratio from 4Mn1Co to 1Mn4Co, metal-oxygen bands changed from Mn-O to Co-O bands, which was consistent with the XRD results.

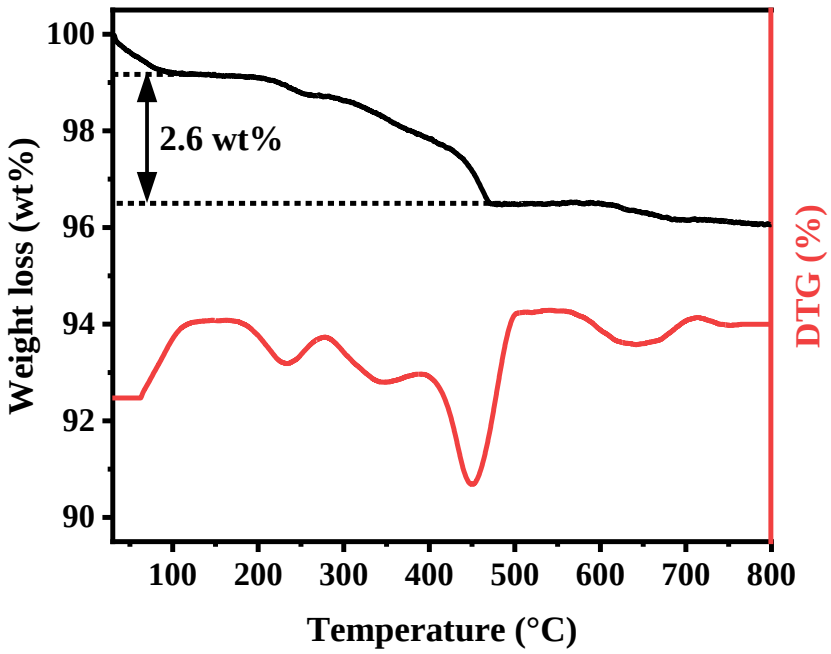

Fig. S4 TG and DTG curves of 2Mn1Co.

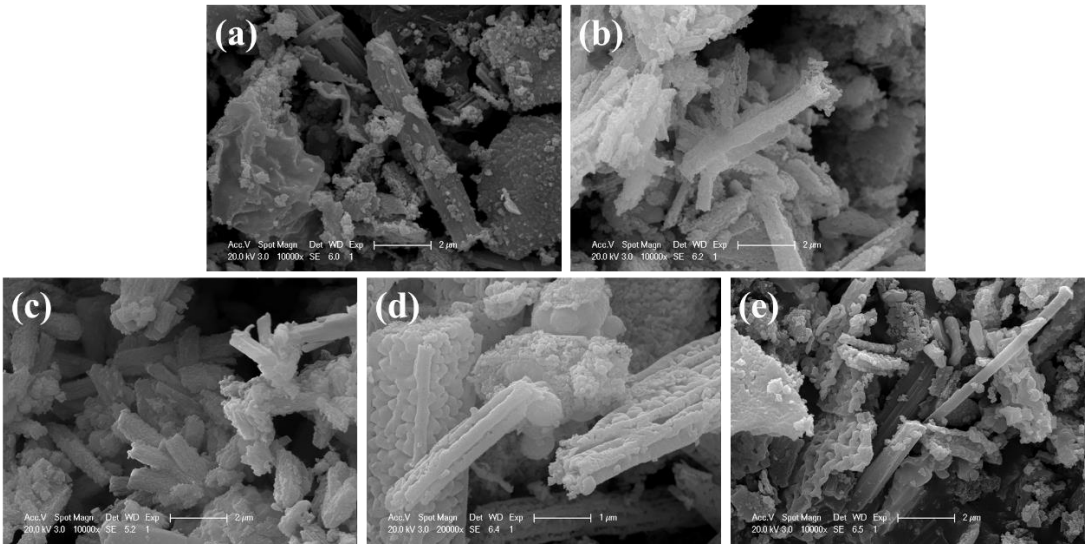

Fig. S5 SEM images of the Mn/Co-MOFs derived MnCoOx catalysts: (a) 4Mn1Co, (b) 2Mn1Co, (c) 1Mn1Co, (d) 1Mn2Co and (f) 1Mn4Co.

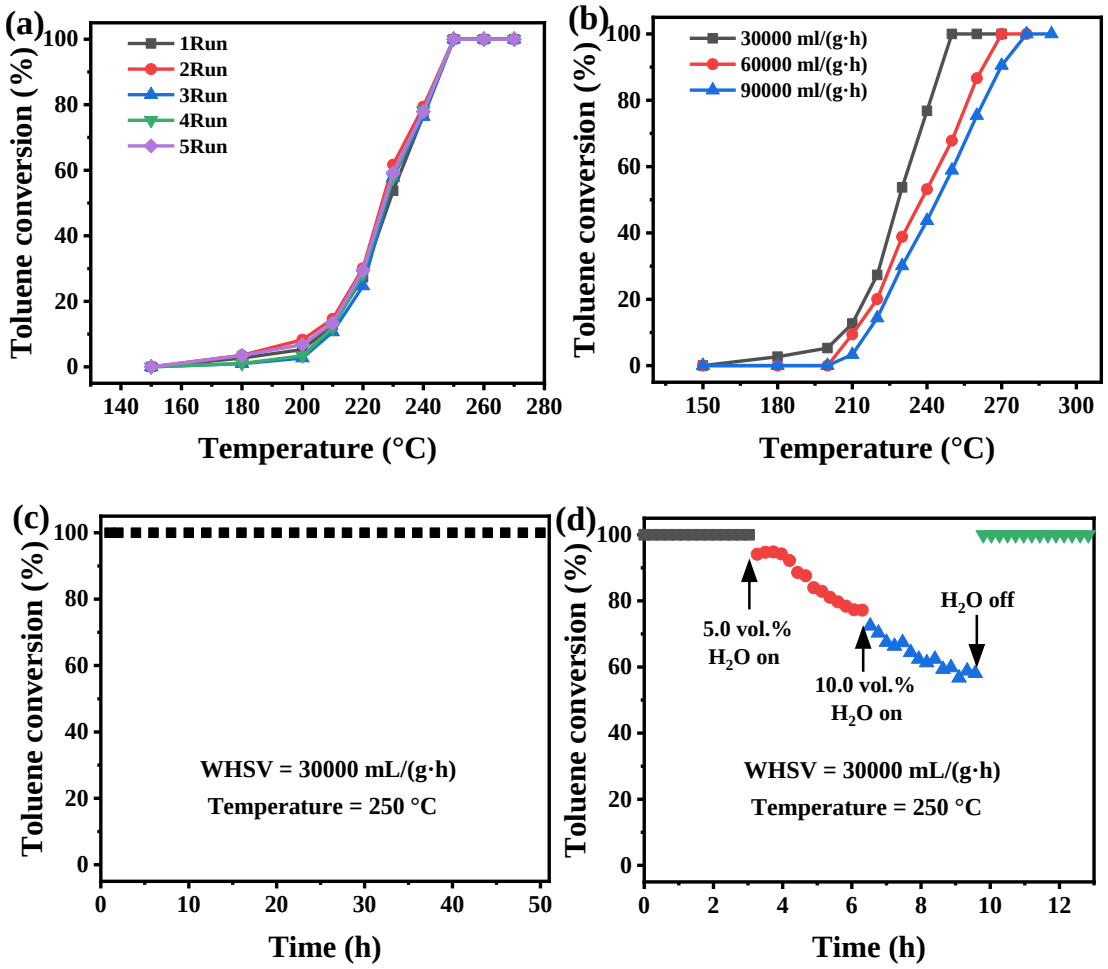

Fig. S6 Reusability (a), effect of WHSV (b), stability test (c), and water-resistance (d) of 2Mn1Co for toluene oxidation.

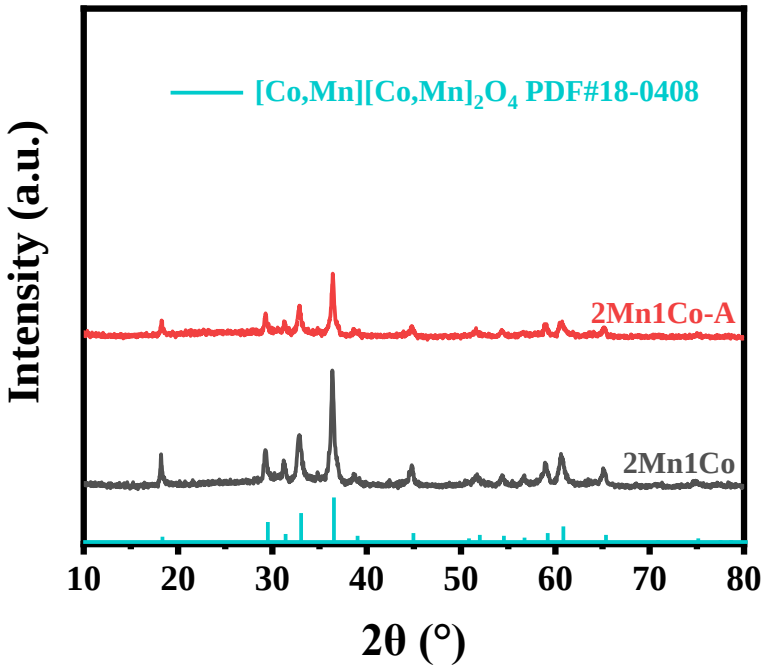

Fig. S7 XRD patterns of 2Mn1Co before and after toluene oxidation.

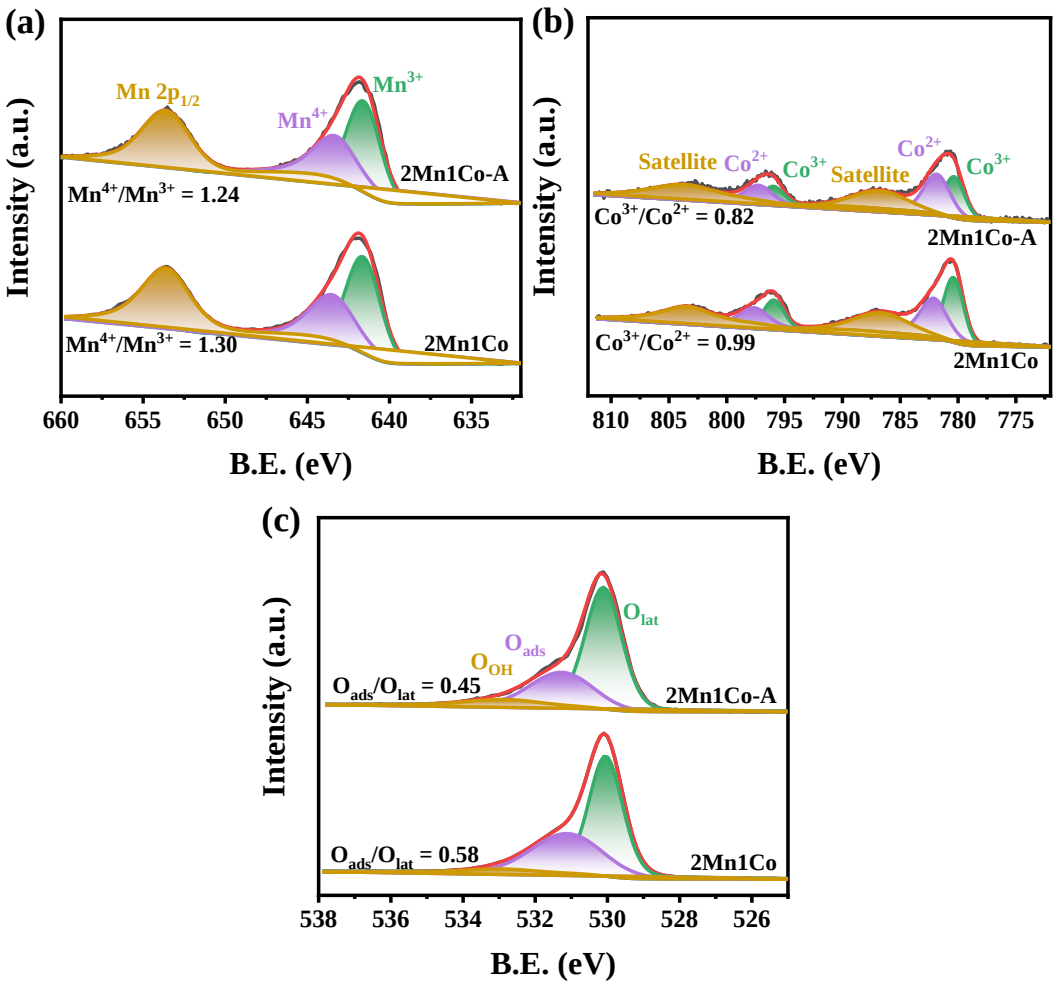

Fig. S8 XPS spectra of 2Mn1Co before and after toluene oxidation: (a) Mn 2p, (b) Co 2p and (c) O 1s orbits.

Ref.

1. F.K. Bi, X.B. Feng, Z.X. Zhou, Y.F. Zhang, J.F. Wei, L.Y.M. Yuan, B.L. Liu, Y.D. Huang and X.D. Zhang, *Chem. Eng. J.*, 2024, **485**, 149776.
2. F.K. Bi, J.F. Wei, B. Gao, N. Liu, J.C. Xu, B.L. Liu, Y.D. Huang and X.D. Zhang, *ACS EST Engg.*, 2024, https://doi.org/10.1021/acsestengg.3c00630.
3. F.K. Bi, X.D. Zhang, J.F. Chen, Y. Yang and Y.X. Wang, *Appl. Catal., B*, 2020, **269**, 118767.
4. J.G. Zhao, P.F. Wang, C.L. Liu, Q. Zhao, J.L. Wang, L. Shi, G.W. Xu, A, Abudula and G.Q. Guan, *J. Colloid Interf. Sci.*, 2023, **629**, 706-722.
5. X. Chen, S.C. Liu, Y. Feng, S. Yang, H.Q. Yu, H.Y. Li, Z.X. Song, W. Liu, M.C. Zhao and X.J. Zhang, *Chemosphere*, 2024, **352**, 141346.
6. L. Luo, R. Huang, W. Hu, Z.S. Yu, Z.X. Tang, L.Q. Chen, Y.H. Zhang, D. Zhang and P. Xiao, *ACS Appl. Nano Mater.*, 2022, **5**, 8232-8242.
7. W. Wang, Y. Huang, Y.F. Rao, R. Li, S.C. Lee, C.Y. Wang and J.J. Cao, *Environ. Sci.: Nano*, 2023, **10**, 812-823.
8. P.F. Wang, J. Wang, X.W. An, J. Shi, W.F. Shangguan, X.G. Hao, G.W. Xu, B. Tang and A. Abudula, *Appl. Catal., B*, 2021, **282**, 119560.
9. P. Liu, Y.X. Liao, J.J. Li, L.W. Chen, M.L. Fu, P.Q. Wu, R.L. Zhu, X.L. Liang, T.L. Wu and D.Q. Ye, *J. Colloid Interf. Sci.*, 2021, **594**, 713-726.
10. W.X. Gu, C.Q. Li, J.H. Qiu and J.F. Yao, *J. Alloys Compd.*,2022, **892**, 162185.
11. K. Awaya, Y. Koyanagi, K. Hatakeyama, J. Ohyama, L.M. Guo, T. Masui and S. Ida, *Ind. Eng. Chem. Res.*, 2021, **60**, 16930-16938.
12. Z. Hu, Z.Y. Tang, T. Zhang, X. Yong, R.L. Mi, D. Li, X. Yang and R.T. Yang, *Ind. Eng. Chem. Res.*, **2022**, 61, 4803-4815.
13. J. Wang, P.F. Wang, A. Yoshida, Q. Zhao, S.S. Li, X.G. Hao, A. Abudula, G.W. Xu and G.Q. Guan, *Carbon Resour. Convers.*, 2020, **3**, 36-45.
14. Y.F. Li, T.Y. Chen, S.Q. Zhao, P. Wu, Y.N. Chong, A.Q. Li, Y. Zhao, G.X. Chen, X.J. Jin, Y.C. Qiu and D.Q. Ye, *ACS Catal.*, 2022, **12**, 4906-4917.

15. F.K. Bi, S.T. Ma, B. Gao, B.L. Liu, Y.D. Huang, R. Qiao and X.D. Zhang, *Fuel*, 2024, **357**, 129833.
16. H. Liu, J.J. Chen, Y. Wang, Q.Q. Yin, W.H. Yang, G.M. Wang, W.Z. Si, Y. Peng and J.H. Li, *Environ. Sci. Technol.*, 2022, **56**, 4467-4476.
17. M.L. Xiao, X.L. Yu, Y.C. Guo and M.F. Ge, *Environ. Sci. Technol.*, 2022, **56**, 1376-1385.
18. F.K. Bi, Z.Y. Zhao, Y. Yang, W.K. Gao, N. Liu, Y.D. Huang and X.D. Zhang, *Environ. Sci. Technol.*, 2022, **56**, 17321-7330.
19. Y. Chen, J. Deng, B. Yang, T.T. Yan, J.P. Zhang, L.Y. Shi and D.S. Zhang, *Chem. Commun.*, 2020, **56**, 6539-6542.
20. S.P. Mo, Q. Zhang, J.Q. Li, Y.H. Sun, Q.M. Ren, S.B. Zou, Q. Zhang, J.H. Lu, M.L. Fu, D.Q. Mo, J.L. Wu, H.M. Huang and D.Q. Ye, *Appl. Catal., B*, 2020, **264**, 118464.
21. S.P. Mo, J. Li, R.Q. Liao, P. Peng, J.J. Li, J.L. Wu, M.Q. Fu, L. Liao and T.M. Shen, *Chem. Eng. J.*, 2021, **418**, 129399.
22. J.Y. Liu, Y.Y. Zhang, X.D. Yan, Z.H. Wang, F.M. Wu, S.M. Feng and P.M. Jian, *Can. J. Chem. Eng.*, 2018, **96**, 1746-1751.
23. H. Liu, X.H. Dai, L.S. Kong, M. Xie, C.J. Sui, Q.Y. Zhang, G. Boczkaj, P. Kowal, B. Cai and J.H. Zhan, *Sep. Purif. Technol.*, 2023, **326**, 124873.
24. Y.H. Chen, A.Q. Luo, D.M. Hu and J.Y. Liu, *Inorg. Chem.*, 2024, **63**, 824-832.